Available online at www.sciencedirect.com

SciVerse ScienceDirect

Ceramics International 39 (2013) 753–761

CERAMICS INTERNATIONAL

www.elsevier.com/locate/ceramint

The PZT system ($PbZr_{1-x}Ti_xO_3$, $0.0 \le x \le 1.0$): Specific features of recrystallization sintering and microstructures of solid solutions (Part 1)

I.N. Andryushina*, L.A. Reznichenko, V.A. Alyoshin, L.A. Shilkina, S.V. Titov, V.V. Titov, K.P. Andryushin, S.I. Dudkina

Research Institute of Physics, Southern Federal University, Rostov-on-Don, Russia Mailing address: 344090 Rostov-on-Don, Stachki ave 194, Russian Federation

Received 23 May 2012; received in revised form 27 June 2012; accepted 28 June 2012
Available online 6 July 2012

Abstract

This work is concerned with the specific features of sintering of solid solutions of the PZT system ($PbZr_{1-x}Ti_xO_3$, $0.0 \le x \le 1.0$) depending on composition. The microstructure of the solid-solution ceramics has been found to be a fairly homogeneous, mosaic, sufficiently close packing of isometric crystallites with a range of section from 3 to 11 μm, but there exists a number of special features related to the component and phase composition of the objects. It has been found that the changes in multifractal parameters of grain structure of these ceramics reflect with high sensitivity the processes of phase transformations in the solid solutions. The obtained results are useful in developing piezoelectric materials based on the PZT system.

Keywords: B. Microstructure; D. PZT; Multifractal parameters; Phase diagram

1. Introduction

The $Pb(Zr_{1-x}Ti_x)O_3$ (PZT) solid solutions find increasing use in various piezoelectric devices. The majority of industrial functional ferro-piezoelectric ceramic materials (FPCM) are based on these solid solutions. Taking into account the fact that the properties of these FPCM's are mainly determined by their crystal structure (which forms at $T=(870–1070)$ K), by their microstructure (which forms at $T=(1070–1370)$ K, i.e., when the structural motive already exists) and by the density of sintered ceramics, it is useful to determine the influence of the composition on the latter as well as on the size of crystallites. This is important from the point of view of determining the correlation between the phase and grain structures of solid solutions as well as due to the possibility of governing the microstructure by varying the composition, i.e., the position of the solid solution on the phase diagram of the system.

2. Objects under study, their synthesis and studying methods

The objects under study are the solid solutions $(1-x)PbZrO_3$- $xPbTiO_3$ $(0.0 \le x \le 1.0)$. In the ranges $0.0 \le x \le 0.12$, $0.30 \le x \le 0.36$, $0.37 \le x \le 0.42$ and $0.52 \le x \le 0.57$ the concentration step, Δx, was 0.01, whereas in the ranges $0.42 < x \le 0.52$ and $0.60 < x < 0.90$ it was 0.005 and 0.0025, respectively.

The samples of solid solutions were prepared according to the conventional ceramic technology (solid-state synthesis, sintering without applied pressure). The synthesis was performed in two stages with intermediate grinding and granulation of the powders. The first and the second annealing temperatures, T_1 and T_2, were 1140 K and 1170 K, respectively. Isothermal ageing at both temperatures was conducted during 7 h. The optimal sintering temperature, T_{sint}, was chosen from three sintering temperatures in the range of (1470–1530) K. The densest sintered samples were obtained at

*Corresponding author: Tel: +78632434066.
E-mail address: futur6@mail.ru (I.N. Andryushina).

0272-8842/$36.00
http://dx.doi.org/10.1016/j.ceramint.2012.06.088

$T_{sint.}$ = (1490–1510)K after 3 h sintering time (depending on composition).

The x-ray studies were carried out by means of the powder diffraction method using the DRON-3 diffractometer (Fe K_α-radiation; Mn-filter; Fe K_β-radiation; Bragg–Brentano focusing scheme). The study was conducted on the bulk and ground ceramic objects, which enabled one to preclude the influence of surface effects, stresses and textures arising in the process of preparation of ceramics. The x-ray density ($\rho_{x\text{-ray}}$) was calculated using the formula: $\rho_{x\text{-ray}} = 1.66 \cdot M/V$, where M is the formula unit weight in grams and V is the perovskite cell volume in Å^3. The homogeneous deformation parameter, δ, was calculated using the following formulae: $\delta = \cos\alpha$ (for the Rh-phase) and $\delta = \frac{2}{3}(\frac{c}{a} - 1)$ (for the T-phase). The measurement errors of structural parameters were estimated to be as follows: $\Delta a = \Delta b = \Delta c = \pm(0.002 \ldots 0.004)$ Å for the linear ones; $\Delta\alpha = 3'$ for the angular ones, and $\Delta V = \pm 0.05$ Å^3 for the volume ($\Delta V/V \cdot 100\% = 0.07\%$).

The experimental density (ρ_{exp}) of the samples was determined by the hydrostatic weighing technique with octane used as the liquid medium. The experimental density was calculated using the formula: $\rho_{exp} = (\rho_{oct} \cdot m_1)/(m_2 - m_3 + m_4)$, where ρ_{oct} is the octane density, m_1 is the mass of the dry sample, m_2 is the mass of the octane-saturated sample, m_3 is the mass of the saturated sample weighed in octane with a suspension, and m_4 is the mass of the suspension for the sample. The relative density (ρ_{rel}) was calculated using the formula $(\rho_{exp}/\rho_{x\text{-ray}}) \cdot 100\%$.

The microstructure examination was carried out in reflected light using the Neophot 21 and Leica DMI 5000 M optical microscopes. The samples were preliminarily ground using fine-grained abrasive paper. Then, a finer grinding was performed by the abrasive having the particle size $D \leq 5$ μm in the presence of aqueous medium. Further polishing was also conducted in the aqueous medium with the Cr_2O_3 powder having the particle size of (0.1–0.2) μm. At the two latter steps the quality of processing was controlled with the help of the microscope (light field and polarized light regimes). The visualization of intercrystalline boundaries of the ferroelectric (FE) ceramics was performed by the chemical etching method using the acidic etchant (5% aqueous solution of the concentrated nitric acid with addition of 15 drops of the concentrated hydrofluoric acid per 200 ml of the etchant), which, depending on the reaction activity of individual materials, could be diluted with water. The etching duration as well as the etchant concentrations were chosen depending on character of the obtained results. The average size of crystallites, $\overline{D}$, was determined by the chord method.

3. Experimental results and discussion

Fig. 1 presents the dependencies of the theoretical (ρ_{theor}), x-ray ($\rho_{x\text{-ray}}$), experimental (ρ_{exp}) and the relative (ρ_{rel}) densities of the PZT system solid solution samples on concentration of the components.

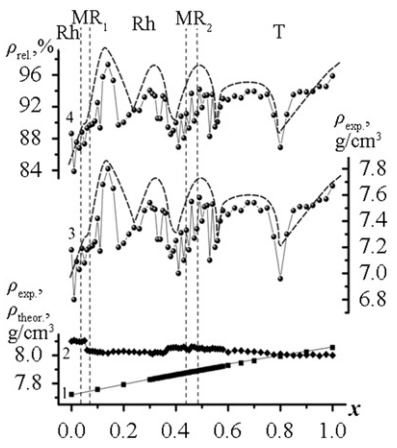

Fig. 1. Concentration dependences of the theoretical (ρ_{theor}) (1), x-ray ($\rho_{x\text{-ray}}$) (2), experimental (ρ_{exp}) (3) and relative (ρ_{rel}) (4) densities of the PZT system solid solution samples.

As can be seen from Fig. 1, the experimental densities have a tendency to increase, like the theoretical ones, but this increase is not monotonous: there are three distinct and one diffuse maxima (see the envelope curve in Fig. 1). The causes of such behavior will be discussed below. The prepared solid solutions possess slightly lowered ρ_{exp} values ($\rho_{exp.aver.} \approx (0.88 \div 0.94)\rho_{x\text{-ray}}$) compared to those of materials prepared by the traditional ceramic technology ($\rho_{exp} \approx 0.95\rho_{x\text{-ray}}$). This is especially typical for the solid solutions from the $PbZrO_3$-rich region ($\rho_{exp.aver.} = 0.85 \div 0.92\rho_{x\text{-ray}}$). Here, the "losses" in ρ_{exp} are as high as ~10%. This effect manifests itself to a lesser degree in the $PbTiO_3$-rich solid solutions having the values of $\rho_{exp.aver.} \sim 0.92 \div 0.94\ \rho_{x\text{-ray}}$. In this case, the "shortage" of ρ_{exp} is 1–3%. This observation may be explained with the following considerations taken into account. According to Ref. [1], the vacancy-diffusion processes dominate in the mass transfer mechanism of oxide materials, to which our objects belong. Let us consider the two end members of the system – $PbTiO_3$ and $PbZrO_3$ – from these positions.

It follows from Ref. [2] that the real $PbTiO_3$ crystal resembles in its structure the intrinsic solid solution, or the autoisomorphic substance [3], a composition of which may be qualitatively described by the formula:

$$Pb_{1-x}\square_x[Ti^{4+}_{[1-(x_2+x_3)](1-z)}Ti^{3+}_z Pb^4_{x_2} Pb^{2+}_{x_3}]O_{3-y}\square_y. \quad (1)$$

here, $x = x_1 + x_2 + x_3$ is the deviation from the PbO stoichiometry, x_1 is the PbO loss resulting from the lead volatility at the temperatures of solid-phase synthesis and sintering, x_2 is the fraction of Pb^{4+} incorporated into the B-sublattice as a result of Pb^{2+} oxidation, x_3 is the fraction of Pb^{2+} incorporated into the B-sublattice, z is the amount of Ti^{3+} being always present in the composition because of its variable valence, y is the originating deficiency in oxygen, and denotes vacancies. This formula does not reflect all the peculiarities of $PbTiO_3$ structure but it shows a considerable difference between the real cationic composition of polycrystals and the ideal $Pb^{2+}Ti^{4+}O_3^{2-}$

structure. Having a lot of vacancies, $PbTiO_3$ easily assumes a required crystal structure and is sintered well.

$PbZrO_3$ is located close to both boundaries of stability of the perovskite structure [4], which is the reason for the easier breaking of Zr–O bonds and decomposition of $PbZrO_3$ into oxides. This is stimulated by the differences in chemical affinity of PbO to the Ti and Zr oxides. In Ref. [5] it was shown that the chemical affinity of PbO to TiO_2 is strong while that to ZrO_2 is weak. Because of the closeness of the $PbZrO_3$ sintering and decomposition temperatures ($\sim$1470 K and T$\sim$1450 K, respectively) the choice of the optimal sintering conditions of ceramics is based on a compromise between these two competing factors, since, from the one hand, it is necessary to increase the temperature in order to reach the maximum density and, from the other hand, one should not allow $PbZrO_3$ to decompose into monooxides. This leads to a "softening" of the preparation conditions of $PbZrO_3$ and, as a result, to the deterioration of its quality.

The concentration range of the PZT system can be divided into three regions in accordance with the crystallochemical composition of solid solutions, imperfection, and, as a consequence, the different sintering activity. The first one is the $PbTiO_3$-based solid solutions ($>70\%$), which are structurally close to $PbTiO_3$ and are sintered well ($\rho_{exp} \geq 95\%\ \rho_{x\text{-}ray}$). It should be noted that in order to avoid self-destruction typical for $PbTiO_3$-based solid solutions [6] they are intentionally obtained with reduced density so that the c/a value of 1.04–1.05 (depending on composition) is not exceeded. Exceeding the upper limit (close to $c/a=1.062$ $PbTiO_3$) results in violation of the integrity of ceramics and their decomposition into individual grains due to internal mechanical stresses arising from the large magnitude and anisotropy of deformation of crystallites [7]. The second region is the $PbZrO_3$-based solid solutions ($>80\%$), which are structurally close to $PbZrO_3$, thermally unstable and require a careful choice of T_{sint} to avoid decomposition. The third (medium) region is the solid solutions with $PbTiO_3$ concentration of $\sim$20–70 M %. In them the peculiarities of crystal structure of pure compounds are not so strongly pronounced (Pb^{4+} ions are not present in them, which is revealed by the light color of ceramics) and the chemical bonding is slightly different despite the large $PbZrO_3$ concentration. These solid solutions are thermodynamically stable and begin to lose PbO appreciably at $T \geq 1520$ K [8], i.e., above the optimal T_{sint} (≤ 1510 K). Because of the larger inhomogeneity in cationic composition (compared to $PbTiO_3$) these solid solutions are sintered not so well as the $PbTiO_3$-based ones ($\rho_{exp} \approx 0.93$–$0.94\%\ \rho_{x\text{-}ray}$) and are less active as evidenced by the small limiting values of their γ-nonstoichiometry described by the formula $A_{1-\gamma}BO_{3-\gamma-\delta}$. For $PbTiO_3$, $PbZrO_3$ and the solid solutions on their basis $\gamma=0.1$, while for those from the middle region $\gamma\sim0.01$–0.015 [9].

The nonmonotonic behaviour of ρ_{exp} and ρ_{rel} with four maxima may be explained by the presence of three morphotropic phase transitions in the system, namely: the rhombic (R)–rhombohedral (Rh), low–high-temperature Rh ($P3m \rightarrow P3c$) and Rh–tetragonal (T) ones at which more favorable conditions for sintering and synthesis are created. The first maximum is slightly shifted to the right of the morphotropic region (MR) because the influence of the "nontechnological" $PbZrO_3$ predominating over the heterophase MR contribution seems to be still strong. A flat maximum in the T region is most likely due to the artificial reduction of T_{sint} because of a tendency of the high-density $PbTiO_3$ to self-destruction.

A calculation of the mean crystallite size ($\overline{D}$) has shown that its x dependence is nonmonotonic (Fig. 2a). One can observe three fairly distinct maxima corresponding to the MR location in the system and a flat maximum in the single-phase T region. The formation of such maxima is, undoubtedly, the result of activation of the diffusion and recrystallization phenomena in the MR due to mobility of all the structural elements: interphase and domain boundaries, vacancies, and so on. These maxima occur at normal conditions (room temperature and $T < T_C$, where T_C is the Curie temperature). In the paraelectric phase, where, strictly speaking, there are no polar states and the microstructure is formed, the changes in $\overline{D}$should not experience the anomalies observed in the experiment. The reason is that in the PZT system the cubic phase is not homogeneous and shows the "memory" effect of the polar phase configuration. This is supported by the fact of nonmonotonic "behaviour" of the unit cell volume at $T > T_C$ and $T >> T_C$ (Fig. 2b) of the solid solutions corresponding to the MR, which indicates a complex character of this phase and the influence of the low-temperature phenomena on the manifestation of different properties of the PZT ceramics far from the phase transition temperature. Similar events "above" the phase transformations were observed earlier in other solid solution systems with morphotropic phase boundaries (MPBs).

In the combined Fig. 3 one can see the changes in $\overline{D}$ and the homogeneous deformation parameter, δ, calculated from the formulae: $\delta = \cos a$ for the Rh phase and

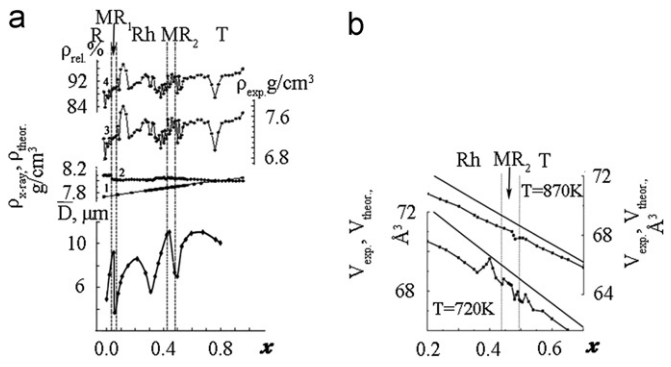

Fig. 2. Concentration dependences of the mean grain size, theoretical (ρ_{theor}) (1), x-ray ($\rho_{x\text{-}ray}$) (2), experimental (ρ_{exp}) (3) and relative (ρ_{rel}) (4) densities (a) and the unit cell volume (b) of solid solutions of the PZT system.

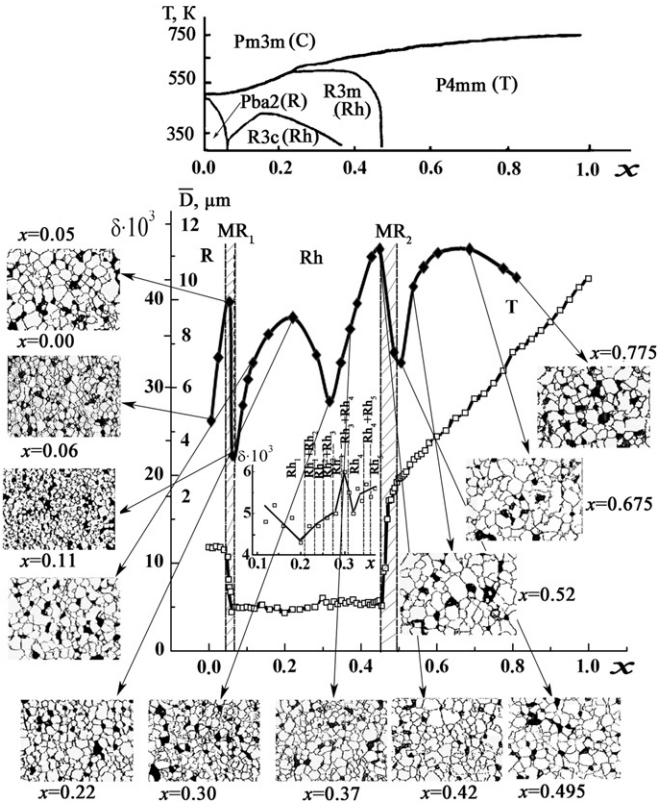

Fig. 3. Variation of the mean grain size, D, and the homogeneous deformation parameter, δ, with the $PbTiO_3$ content in the PZT system. The phase diagram is taken from Ref. [32]. The symmetries are designated as R (rhombic), Rh (rhombohedral), T (tetragonal); MR_1 and MR_2 denote morphotropic regions.

$\delta = \frac{2}{3}\left(\frac{c}{a}-1\right)$ for the T phase [10]. The central parts of the dependences of δ inside the MR were obtained by summing up δ of the coexisting phases using the lever rule. It can be seen that in a wide range of chemical and phase compositions of solid solutions the $\overline{D}$ and δ values are inversely dependent, i.e., the maximum of $\overline{D}$ corresponds to the minimum of δ (in the MR). Similar situation takes place, also, in other systems (in multicomponent PZT-based and simpler ones based, for example, on $NaNbO_3$) upon variation of concentration of the components or technological regulations [11]. Low δ values in the MR evidence of more favourable conditions for the diffusion processes, the mass transfer and the recrystallization sintering. At such conditions, even a negligible change in the cationic composition substantially affects the formation of microstructure of the samples leading to an abrupt enlargement of crystallites in the MR, which we observe experimentally.

These results seem contradictory in view of the fact that the assessment of δ is made at $T < T_C$ where independent crystalline forms of different symmetry and the regions of their coexistence retain, whereas the perfection of the grain structure is performed at $T \geq T_C$ in the cubic nonpolar phase, where there are no MR by definition.

However, as noted in Ref. [12], because of the difference in cohesion characteristics (formation heat, entropy, enthalpy, interaction parameters of the components, internal lattice energies, and so on) of $PbTiO_3$, $PbZrO_3$ and their solid solutions due to the interatomic and intermolecular interactions of different nature, one can expect their serious influence on the character of physical processes governing the structural transitions and the peculiarities of different physical properties related to them. In Ref. [13] such interactions were assigned only a negligible role, with which the changes in parameters of the microscopic processes occurring in the crystals are connected. The influence, however, may be more substantial as evidenced by the following facts concerning the PZT system and reported in Refs. [14–17]. The activity of lead oxide at $T < 1130$ K, including the T phase, is not a linear function of composition as it might be expected in the case of a regular solid solution [14]. In the $PbZrO_3$-rich region, $T_C(x)$ possesses a "plateau", which is an indication of structural transformations in the system [9]. Near the MPB (Rh → T), at long (one year) ageing times, the poled single-phase solid solutions break down into two coexisting ones of Rh and T modifications, i.e., in essence, there appear local regions of insolubility of the components [16]. The experimentally determined (using the calorimetry of melted oxide solutions at high temperature, $T = 973$ K) in Ref. [17] value of the formation heat of PZT solid solutions from the constituent oxides (PbO, ZrO, TiO_2) does not correspond to the calculated one in the approximation of regular solid solutions due to the unexpectedly large interaction parameter ($W = 40 \pm 4.7$ kJ/mole). In Ref. [12] a complex behaviour of the PZT solid solutions in the high-symmetry (cubic) phase was determined and a direct support for this comes from following. The enthalpy of transition to the T phase increases linearly with the $PbZrO_3(x)$ content in the system, while in the Rh phase it is independent of x and remains constant in the range $0.52 \leq x \leq 0.95$. With the increase of $PbTiO_3$ concentration, at $x = 0.35$, the signs of the Coulomb energy, ΔE_M, and the short- range repulsive force, ΔE_N, change (ΔE_N is due to the repulsion of electron shells of the ions and begins to act when the atoms are brought closer to each other). This evidences of the "softening" of the repulsive energy with respect to other contributions to the lattice energy. In the cubic phase, the data reveal "traces" of differing Ti and Zr displacements typical of the low-symmetry phases, which is explained, in part, by the differences in characteristics of hybridization of d-states of the chemical Ti–O and Zr–O bonds. A drastic change in the temperature dependence of x–ray line widths at the Curie point was discovered: the cubic reflection 200 increases in width with decreasing temperature down to T_C, while the width of the T profiles 200 and 002 decreases below T_C, with the T reflections 200 being considerably broader than the reflections 002. The changes in the total enthalpy of transitions are ~2–3 kJ/mole, which indicates the energetics of a well-balanced system.

It follows from what was said above that there is a significant influence of the cohesion properties on the character of the FE phase transition, with the influence being more pronounced near the MPB. As shown in Ref. [12], in the low-symmetry FE phases one can observe the following phenomena: a strong correlation of the ferroelastic distortion ($c/a-1$) and, hence, of the spontaneous deformation with the magnitude of ΔE_N in the T phase, while in the Rh phase this correlation is absent; compositions with large Δa ($\Delta a = a_{exp} - a_{theor}$, where a is the cell parameter) have smaller $c/a-1$ values, though when taking account only of the geometrical sizes one could expect a direct dependence $\Delta a = f(c/a-1)$; the above-mentioned dependence of $c/a-1$ on ΔE_N does not promote large distortions of the T cell of PZT solid solutions; at $x<0.7$ nonuniform displacements of octahedral Ti and Zr cations take place, namely: the Ti displacements increase quickly, while the Zr ones tend to zero. Such a difference in the rates of ionic displacements may be one of the factors provoking a tendency of phase separation; in the T phase the lattice parameter c is weakly dependent on x, while the parameter a increases steadily. This fact rather supports the existence of a nonuniform ionic displacement than is a consequence of composition fluctuations Δx. In Ref. [18] it is suggested that the ionic displacements have, at least, two scales of correlation lengths: one connected with local distortions, and the other connected with the order parameter. This explains the fact that even in the pure $PbTiO_3$ the phase changes behave not in the way expected for a pure displacive ferroelectric and are retained in the paraelectric region [19,20]. Thus, a complex behaviour of the PZT solid solutions in the cubic phase could explain the observed anomalies in physical properties, including those in the character of paraelectric to ferroelectric phase transitions. Since the vibrational density of states is related to the bond configuration, the above-mentioned imperfections (nonideality) of the cubic solid solutions should affect the displacement character [12].

There is a further point to be made. Not only the "events" taking place in the low-symmetry phases find response in the paraelectric phase, but also the high-temperature states favouring certain processes can, as a "memory effect", manifest themselves at normal conditions. The essence of this effect is as follows: if a necessary concentration of anion vacancies is created in the material, then arising local stresses are able to maintain the high-temperature states even at room temperature [21–23].

Fig. 4 shows typical fragments of microstructure of the PZT ceramics of various compositions belonging to different parts of the phase diagram. It is seen that, as a whole, their microstructure is a fairly homogeneous, mosaic, sufficiently close packing of isometric crystallites of 3–11 μm in section (Fig. 4). On approaching $PbTiO_3$ the real porosity increases and the size of intercrystalline contact areas decreases (in this case, a tendency to minimize the surface energy leads to formation of the more rounded type of crystallites) (Fig. 5). It should be noted that, in this case the observed porosity is overstated compared to the real one because of the grain losses arising during grinding and polishing, which leads to the structure loosening.

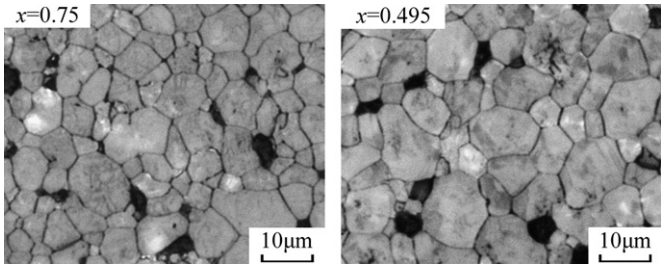

Fig. 4. Fragments of the PZT ceramics ($x=0.75$, 0.495). Magnification: 1000x.

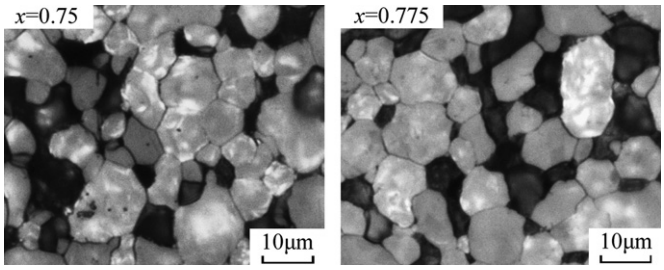

Fig. 5. Fragments of the PZT ceramics ($x=0.75$, 0.775). Magnification: 1000x.

A specific feature of grain structure of the PZT ceramics is the difference in sizes, packing and degree of perfection of the crystallites around the pores (comparable with them and large ones) and far from the pores. Large pores are surrounded by a layer (or layers) of closely packed, defect-free large crystallites having the shape close to idiomorphic, while the small, loosely packed and less perfect crystallites grow far from the pores. Such sphere-like ("flower-type") structures in the form of clusters "one pore—single- or multi-layer grain shell" are usually statistically uniformly distributed in the main, more often, finer-grain matrix of dense ceramics (Fig. 6a). When their number increases they start to order to produce extended formations in a form of a single (Fig. 6b) at first and then numerous (Fig. 6c) columns, which in some cases cover large areas with a radial-circular net of boundaries (Fig. 6d).

Such inhomogeneities arise due to the following reasons. The large pores playing a role of drains for vacancies and dislocations in the process of recrystallization promote the growth of the defect-free crystallites near themselves as well as the appearance of the clusters described above. Facilitation of interaction of the latter in a loose structure results in their ordering. Similar phenomenon was observed in the porous $NaNbO_3$ ceramics [24].

In the vicinity of the MR one observes a violation of the homogeneous distribution of grains in the volume of the

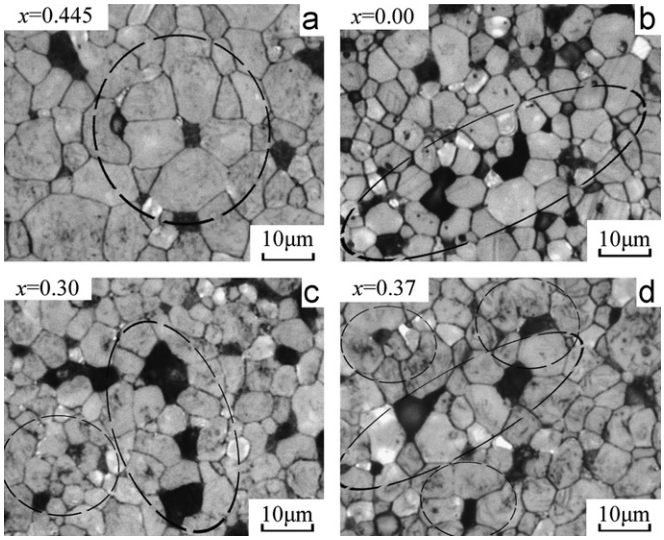

Fig. 6. Fragments of the PZT ceramics (x=0.00, 0.30, 0.37, 0.445. Magnification: 1000x.

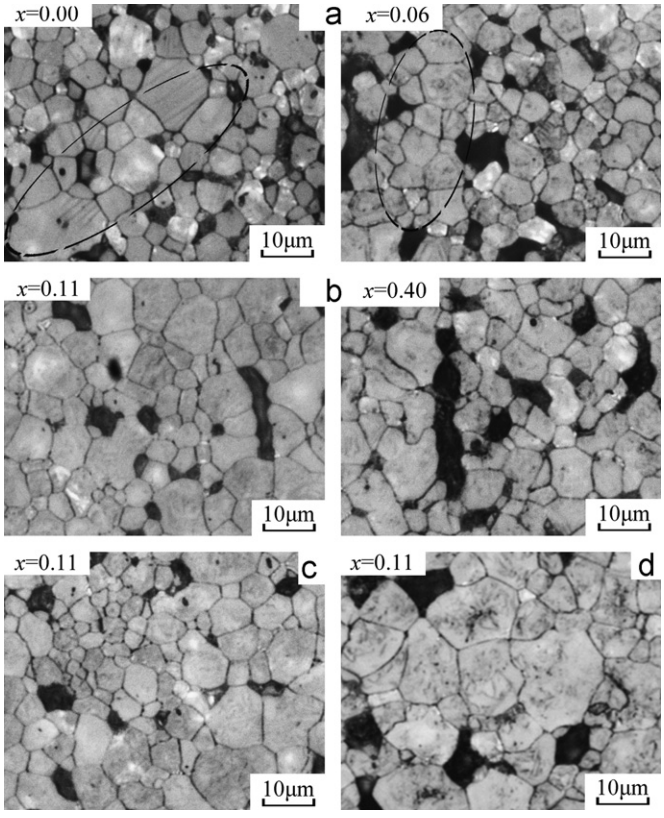

Fig. 7. Fragments of the PZT ceramics (x=0.00, 0.06, 0.11, 0.40). Magnification: 1000x.

sample: there appear "chains" of large crystallites (Fig. 7a), pore channels (Fig. 7b), "colonies" of small grains against a background of the larger matrix ones (Fig. 7c), and the regions with extremely curved grain boundaries (Fig. 7d), which may be the result of structure clusterization when, far from the MR, in the entrails of the single-phase area, there appear the nuclei of another phase and the structure becomes, in essence, heterogeneous. Similar effect was described in Ref. [25].

When the normal growth of grains in the polycrystalline material ends, one can often observe another type of recrystallization. Some grains grow without difficulty at the expense of the others (Fig. 8) and may reach giant sizes (Fig. 9), while the size of the main grain mass remains practically unchanged. This phenomenon is known under the name of discontinuous secondary recrystallization [26]. Such an excessive growth of grains at the expense of absorption of the smaller ones can occur locally (Fig. 8a) or cover rather vast areas (Fig. 8b). In this case one observes another effect—a capture of pores by the large grains leading to the formation of intragrain porosity (Fig. 9). This recrystallization may occur if there is a grain possessing larger number of facets than that of the mean size grain. Then, owing to the large number of facets, the curvature of local boundaries increases and, thus, the driving force giving rise to migration (proportional to this curvature) increases as well. If the size of this grain reaches the critical value [27], the boundaries can overcome the resistance of pores or inclusions and renew the migration in the direction of the main polycrystalline mass where the growth of crystallites has already stopped. Since the boundaries of these large grains move very quickly, the time available for annihilation of the excess vacancies surrounding the pores is, usually, too short for the complete removal of pores. Moreover, now the boundary passes through the pore only once and, therefore, the pores are captured inside large grains. Often, this state indicates the end of sintering. The remaining few boundaries

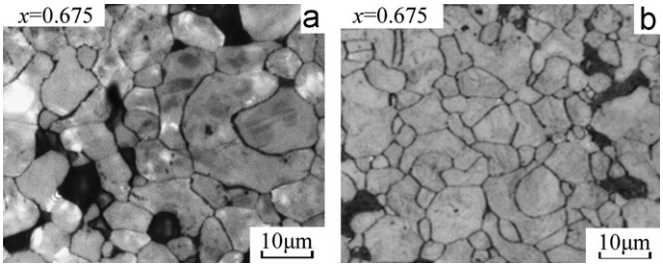

Fig. 8. Fragments of the PZT ceramics (x=0.675). Magnification: 1000x.

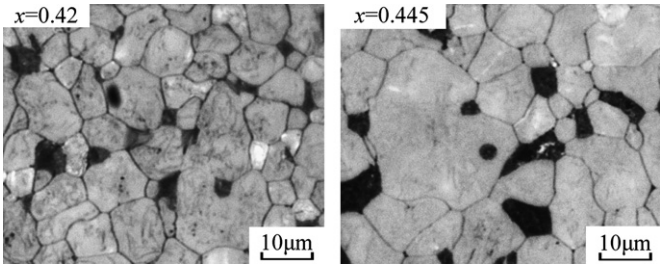

Fig. 9. Fragments of the PZT ceramics (x=0.42, 0.445). Magnification: 1000x.

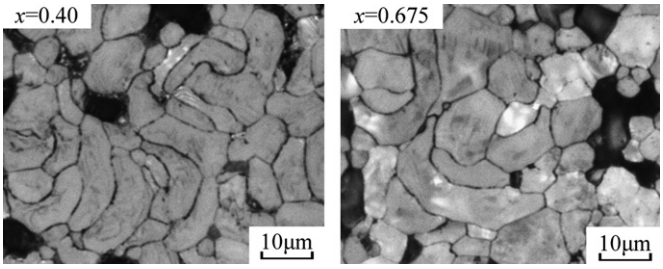

Fig. 10. Fragments of the PZT ceramics ($x=0.40$, 0.675). Magnification: 1000x.

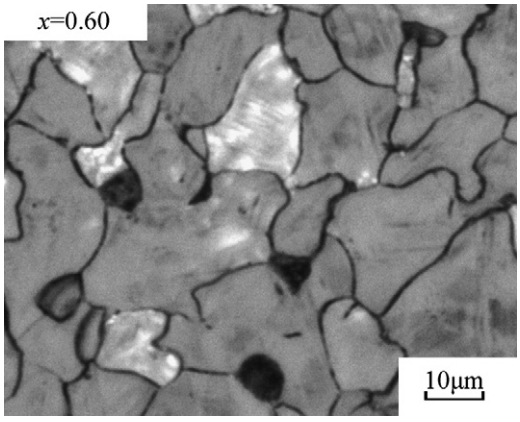

Fig. 11. Fragments of the PZT ceramics ($x=0.60$). Magnification: 1000x.

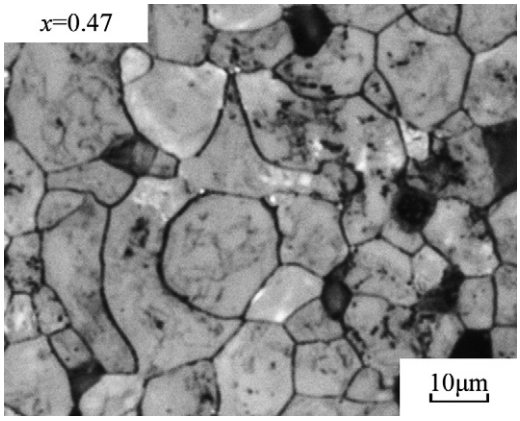

Fig. 12. Fragments of the PZT ceramics ($x=0.47$). Magnification: 1000x.

between the large grains migrate so slowly that subsequent removal of pores becomes technologically inexpedient.

At the local overheating of the samples (because of the temperature gradient existing in the ovens) there may form grains with very unusual boundary shapes, which most often crystallize in the surface layer. Such regions may have different extensions (Fig. 10). In the case of "global" overheating ("oversintering") of the samples one can observe completely melted grains presented in Fig. 11.

All the above-mentioned anomalies in the grain structure of the PZT ceramics are often present simultaneously, as if they "attract" each other (Fig. 12), and form areas of abnormal grain growth.

A detailed study of grain structures was also carried out by means of their multifractal parameterization [28]. The $f(\alpha)$-spectra and the spectra of the generalized dimensions (Renyi dimensions), D_q, were analyzed for the approximated black-and-white images of microstructures of the samples under study. The D_q spectra and the $f(\alpha)$-spectra were determined in accordance with the standard interpretation of the multifractal formalism [28] from Eqs. (2)–(5):

$$\tau(q) = \lim_{\varepsilon \to 0} \frac{\ln \sum_{i=1}^{N} \mu_i^q}{\ln \varepsilon}, \tag{2}$$

$$\alpha(q) = \frac{d\tau}{dq}, \tag{3}$$

$$f(\alpha) = q\alpha - \tau, \tag{4}$$

$$D_q = \frac{\tau}{q-1}, \tag{5}$$

where $\{\mu_i\}$ is the measure introduced in Ref. [28]. This measure is generated at equal-cell discretization of the Euclidean space, which contains the object under study, into N cells of size ε. The measure is determined for all the cells of the discretization. To each cell containing a grain boundary element the weight value $\mu_i \neq 0$ is assigned so that the condition (5) is fulfilled:

$$\sum_{i=1}^{N} \mu_i = 15 \tag{6}$$

The weight of the cell not containing any boundary is $\mu_i = 0$.

For calculations, only the canonical spectra were used [29], that is the spectra satisfying the following conditions: $Dq1 \geq Dq2$ for $q1 \leq q2$, and $f(\alpha(q=0)) = \text{maximum} = D_0$, $f(\alpha(q=1)) = \alpha(q=1) = D_1$ and $f(\alpha(q1)) \leq f(\alpha(q2))$, $\alpha(q1) \alpha(q2)$ for $q1 \geq q2 \geq 0$. For parameterization the following parameters of canonical spectra were used as the most informative: the fractal dimension, D_0; the parameter of "homogeneity", $f_\infty = f(\alpha(q))$, at $q \gg 1$, being an indicator of the distribution character of the unit structural elements in the Euclidean space containing this structure (in the calculations of $f(\alpha(q))$ for $q \gg 1$ the q parameter value was set to 40); and the "order" parameter, $\Delta_\infty = D_1 - D_q$, at $q \gg 1$, being the degree of symmetry breaking of the measure of the studied structure with respect to the multifractal transformation [28]. Here, D_1 (the value of D_q at $q=1$) is the value of information dimension defined by Eq. (7) as a result of evaluation of the indeterminate form in Eq. (5) at $q \to 1$:

$$D_1 = \lim_{\varepsilon \to 0} \frac{\sum_{i=1}^{N} \mu_i \ln(\mu_i)}{\ln \varepsilon} \tag{7}$$

In calculating D_q for $q \gg 1$ the q parameter value was also assumed to be equal to 40 [28–30].

By definition the fractal dimension D_0 is related to the grain boundary shape as well as (according to Ref. [30]) to the degree of self-similarity of sections of the grain boundaries. The minima of the "homogeneity" parameter correspond to maximum values of microdeformations in the crystal structure. The maxima of the "order" parameter, related, by definition of the information dimension (D_1), to the entropy of the system of grain boundaries (Eq. (7)) and to the spatial correlation of distribution of the structural elements (D_∞), correspond to the states with the most stable distributions of the forms and sizes of ceramic grains in space [31].

The main tendency of changes in the microstructure of the PZT ceramics in the region of the AFE→FE phase transition with increasing Ti concentration is clearly evident from Fig. 13a. The regular faceting of large grains of the monoclinic AFE phase is replaced after the phase transition by a more incised fine-grained microstructure. This tendency in evolution of the grain structure is numerically confirmed by the obtained values of the fractal dimension D_0.

As shown in Fig. 13b, in the beginning of the formation of solid solutions the grain surface decreases and then increases step-wise at the transition to the FE state; the return of the values to the $PbZrO_3$ level occurs only far from the phase transition region at $x \approx 0.20$. The behaviour of the "homogeneity" parameter f_∞ (Fig. 14) shows that small Ti

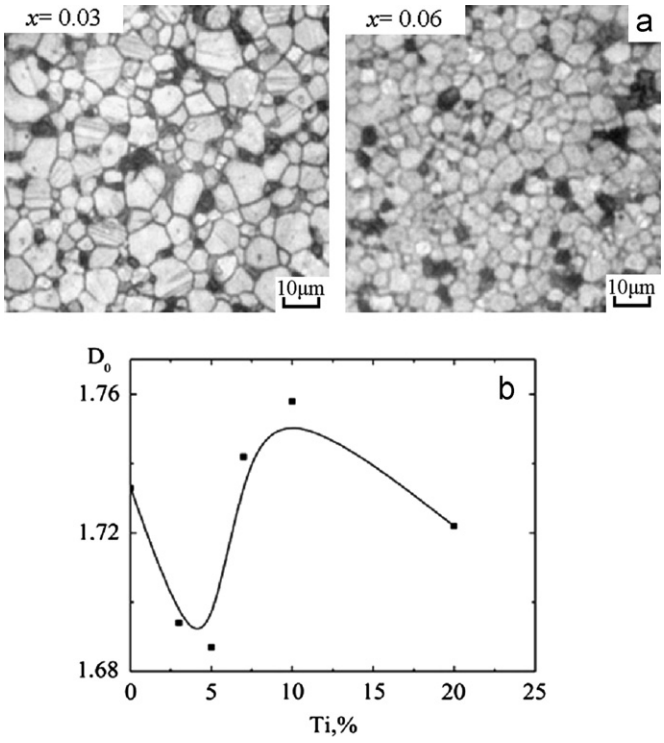

Fig. 13. Changes in the character of microstructure at the transition from the AFE ($x=0.03$) to FE ($x=0.06$) region (a) and the fractal dimension D_0 at increasing Ti concentration in the PZT ceramics (b).

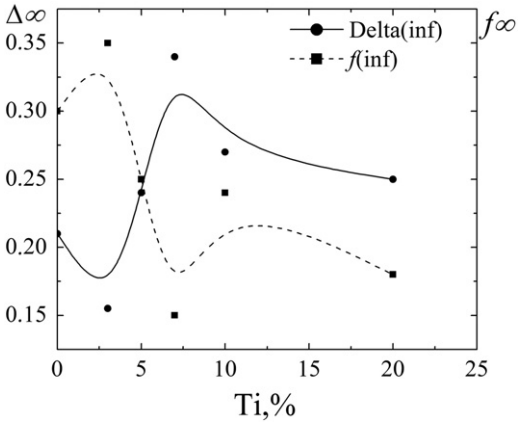

Fig. 14. Changes in the homogeneity parameter, f_∞, and the order parameter, Δ_∞, at increasing Ti concentration in the PZT ceramics.

concentrations in solid solutions (up to 3 at.%) promote relaxation of mechanical stresses leading to the growth of the mean size of grains and flattening of their boundaries.

However, already at $x=0.05$ one can observe a rapid growth of stresses and a drastic enhancement of the "long-range" structure correlations in the ceramic object. This is evidenced by the decrease of f_∞ and increase of Δ_∞. It should be noted that at the same time the decrease of D_0 continues, which indicates further growth of grain sizes and flattening of the grain form. Such behaviour of multifractal parameters is, undoubtedly, a special feature of the microstructure in the region of the phase transition under study. This particular state of the grain structure arising in the process of recrystallization may be one of the factors promoting the coexistence of the AFE and FE phases in solid solutions with $0.04 < x < 0.06$. The subsequent behaviour of multifractal parameters is typical of phase transformations in the ferro-piezoelectric ceramics. The central point is the fact that the level of microstresses in the structure in the whole FE region under study is considerably higher than in the AFE one and the microstresses increase with Ti concentration in the PZT solid solutions.

To summarize, the changes in multifractal parameters of grain structure of the PZT ceramics evidence with high sensitivity of the processes of phase transformations in the solid solutions.

4. Conclusions

The results of the study of the specific features of sintering of solid solutions depending on their composition can be summarized as follows.

(1). Lower density values are peculiar to the end members of the system, which is connected with their crystallo-chemical features (practical absence of vacancies in the structure, thermal instability of $PbZrO_3$, and strong mechanical stresses in $PbTiO_3$ because of the large magnitude and anisotropy of deformation of the

crystallites leading to its self-destruction). The nonmonotonic change in the density (ρ_{exp}) with the maxima at certain x values is related to localization of the vacancy-saturated morphotropic regions (R→Rh, Rh→T) and of the region of diffuse R3c→R3m phase transition, inside which there occur favourable conditions for diffusion and mass transfer in the process of synthesis and sintering. The spread of values of ρ_{exp} in the Rh region is related to the large number of structural rearrangements in this concentration range.

(2). Microstructure of the solid solution ceramics is, as a whole, a fairly homogeneous, mosaic and sufficiently close-packing of isometric crystallites of 3–11 μm in section. However, there is a number of special features related to the component and phase composition of the objects, such as the formation of sphere-like structures in the form of clusters such as "one pore—single- or multi-layer grain shell", "chains" of large grains, including the repeatedly recrystallized ones, "channels" of pores, "colonies" of extremely small grains, areas of abnormal grain growth, etc., and the nonmonotonic change in D- similar to the $\rho_{exp}(x)$ dependence.

(3). The changes in the multifractal parameters of grain structure of the PZT ceramics evidence with high sensitivity of the processes of phase transformations in the solid solutions.

These results may be helpful in developing piezoelectric materials based on the PZT system.

Acknowledgements

We appreciate the help of Nikita Ter-Oganessian with the preparation of the manuscript. This work was financially supported by the Ministry of Education and Science of the Russian Federation, State contract 16.513.11.3032.

References

[1] Yu.D. Tretiakov, Tverdofaznie Reakcii, Chemistry, Moscow, (1978). (In Russian).
[2] S.V. Titov, L.A. Shilkina, O.N. Razumovskaya, L.A. Reznichenko, V.G. Vlasenko, A.T. Shuvaev, S.I. Dudkina, A.N. Klevtsov, Inorganic Materials 37 (7) (2001) 718–725.
[3] G.B. Bokii, Vvedenie v krystallohimiu, Izdatelstvo MGU, Moskow, (1954). (In Russian).
[4] N.G. Leontiev, V.G. Smotrakov, E.G. Fesenko, Physics of the Solid State 25 (7) (1983) 1958–1964.
[5] K.Okazaki, Tehnologiya keramicheskih dielectrikov, Perevod s yaponskogo, Energia, Moskow, (1976). (In Russian).
[6] B. Noheda, J.A. Gonzalo, L.E. Cross, R. Guo, S.E. Park, D.E. Cox, G. Shirane, Physical Review B 61 (2000) 8687–8695.
[7] E.I. Bondarenko, V.D. Komarov, L.A. Reznichenko, V.A. Chernishkov, Sov. Phys., Technical Physics **33** (1988) 1071.
[8] D.Ya. Yanson, K.I. Bindar, O.S. Maksimova, R.Sh. Freidenfeld, Bulletin Academy Science USSR. Series Inorganic Materials 2 (9) (1966) 1563–1567.
[9] L.A. Reznichenko, L.A. Shilkina, O.N. Razumovskaya, O.Yu. Kravchenko, V.V. Akhnazarova, Crystallography Reports 51 (1) (2006) 87–95.
[10] E.G. Fesenko, Semeistvo perovskita i segnetoelectrichestvo, Atomizdat, Moskow, (1972). (In Russian).
[11] A.Ya. Dantsiger, L.A. Reznitchenko, S.I. Dudkina, O.N. Razumovskaya, L.A. Shilkina, Ferroelectrics 214 (1998) 255–259.
[12] G.A.Jr. Rossetti, J.P. Cline, Y.-M. Chiang, A. Navrotsky, Journal of Physics: Condensed Matter 14 (2002) 8131–8143.
[13] V.E. Yurkevich, B.N. Rolov, Physica Status Solidi B 52 (1) (1972) 335–343.
[14] K.H. Hardtl, H. Rau, Solid State Communications 7 (1) (1969) 41–45.
[15] A. Amin, R.E. Newnham, L.E. Cross, Materials Research Bulletin 15 (1980) 721–728.
[16] K. Kakegawa, J. Mohri, S. Shirasaki, K. Takahashi, Journal of the American Ceramic Society 10 (1982) 515.
[17] M. Rane, A. Navrotsky, G.A.Jr. Rossetti, Journal of Solid State Chemistry 161 (2001) 402–409.
[18] G.A.Jr. Rossetti, A. Navrotsky, Journal of Solid State Chemistry 144 (1999) 188–194.
[19] T. Miynaga, K. Sato, S. Ikeda, D. Diop, Geotechnical Engineering Environmental Challenges (2002) 792–800.
[20] K. Sato, T. Miynaga, S. Ikeda, D. Diop, Physica Scripta 115 (2005) 359–361.
[21] V.I. Alexeenko, G.K. Volkova, Technical Physics 70 (9) (2000) 1154–1158.
[22] F. Mupton, R. Roy, Journal of the American Ceramic Society 43 (1960) 234–240.
[23] V.B. Glushkova, Redkozemelnie Metlalli, Splavi i Soedineniya, Nauka, Moscow, 1973 In Russian.
[24] V.V. Akhnazarova, V.D. Komarov, O.N. Razumovskaya, L.A. Reznichenko, L.A. Shilkina, S.I. Dudkina, V.V. Gershenovich, Russian Physics Journal 52 (9) (2009) 957–964.
[25] S.V. Titov, L.A. Shilkina, L.A. Reznichenko, S.I. Dudkina, O.N. Razumovskaya, S.I. Shevtsova, E.M. Kuznetsova, Technical Physics Letters 26 (9) (2000) 810–813.
[26] K. Kui, I i Sbornik II, Conferencii Britanskogo i Golandskogo keramicheskogo obshestv. Perevod s angliiskogo Izd. "Metallurgia". Moskow (1967) 228 In Russian.
[27] J.E. May, D. Turbull, Transactions Metals Society AIME 212 (1958) 769–781.
[28] G.V. Vstovsky, Foundations of Physics 27 (10) (1997) 1413–1444.
[29] G.V. Vstovsky, A.G. Kolmakov, I.Sh. Bunin, Moskow- Izhevsk, NIC «Regularnaya i haoticheskaya dinamica» (2001) 116 In Russian.
[30] V.V. Titov, S.V. Titov, L.A. Reznichenko, O.N. Razumoskaya, L.A. Shilkina, Bulletin of the Russian Academy of Sciences Physics 69 (7) (2005) 1046–1048.
[31] V.V. Titov, S.V. Titov, L.A. Reznichenko, Fizicheskay Mezomechanica 7 (1) (2004) 275–278 In Russian.
[32] V.V. Eremkin, V.G. Smotrakov, V.G. Fesenko, Physics of the Solid State 31 (6) (1989) 156.